Published in final edited form as:
J Glaucoma. 2012 February ; 21(2): 95–101. doi:10.1097/IJG.0b013e31820bcfbe.

Correlating RNFL Thickness by OCT with Perimetric Sensitivity in Glaucoma Patients

Joe L. Wheat, OD, **Nalini V. Rangaswamy, PhD**, and **Ronald S. Harwerth, OD, PhD**
College of Optometry, University of Houston, Houston, Texas USA

Abstract

Purpose—To determine whether a structure-function model developed for normal age-related losses of retinal ganglion cells also models the retinal ganglion cell losses in glaucomatous optic neuropathy.

Methods—The model to relate age-related loss of retinal nerve fiber layer thickness and reduced sensitivity for standard automated perimetry was evaluated with data from thirty glaucoma patients and forty normal subjects. Perimetry thresholds were translated into separate retinal ganglion cell body estimates for test locations in the superior and inferior visual field. The retinal nerve fiber layer thickness from optical coherence tomography was also divided into regions representing the superior and inferior hemifields to obtain the nerve fiber layer area for estimates of the axons in each hemifield. The two estimates of retinal ganglion cell populations were compared for corresponding regions.

Results—Agreement between neural estimates was good for normal subjects and patients with early glaucomatous damage. Results for subjects with advanced glaucoma showed disparities between neural estimates that were proportional to the stage of disease. A correction factor for the stage of disease was introduced for the derivation of retinal ganglion cell axon populations from the retinal nerve fiber layer thickness measurements which produced agreement between the optical coherence tomography and perimetric estimates for all patients.

Conclusions—The modified structure-function model provided well-correlated relationships between the subjective measures of visual sensitivity and the objective measures of retinal nerve fiber layer thickness when parameters for the patient's age and the severity of the disease were included. The results suggest constitutive relationships between structure and function for the full spectrum of normal eyes to eyes with advanced glaucomatous neuropathy.

Keywords

glaucoma; optical coherence tomography; perimetry; retinal ganglion cells; retinal nerve fiber layer

Introduction

Glaucomatous disease is usually diagnosed and managed with measurements of the structural and functional alterations associated with the losses of retinal ganglion cells (RGCs) and their axons. Although, functional measures, such as standard automated perimetry (SAP), have been the gold-standard for glaucomatous neuropathy, high-resolution imaging has excellent accuracy and precision for assessment of structural defects caused by glaucoma, especially the thinning of the RNFL.[1–4] In theory, the clinical procedures should

Corresponding author and address for reprints: Joe L. Wheat, University of Houston, 505 J. Davis Armistead Bldg. Houston, TX 77204-2020 USA, Telephone: 713-743-3325, FAX: 713-743-2053, jwheat@optometry.uh.edu.

provide complementary assessments of glaucomatous neuropathy but comparisons of the two approaches have reported discrepancies in the time-courses of structural and functional defects.[5–7] In some instances, it appears that structural losses precede functional losses (pre-perimetric glaucoma),[4, 8–10] while other investigations have suggested a period of RGC dysfunction prior to detectable structural alterations caused by RGC death.[11–13] However, it seems more likely that there is an overall correlation between structure and function in glaucomatous disease because the underlying changes in both are caused by losses of RGCs.[9, 10, 14]

A number of factors might confound the direct comparison of SAP sensitivity to RNFL thickness. First, the two instruments have very different dynamic ranges of measurements: SAP measures visual sensitivity over a 4 log unit range,[15] whereas RNFL thickness is measured over a linear range of approximately 25 to 200 microns in normal individuals.[16–18] Second, in order to compare localized defects in the RNFL thickness with SAP threshold values, one must adopt a topographical map that relates the perimetric test location's origin in the retina to the corresponding location where it would have its axons enter the optic nerve head.[7, 19–21] Few investigations into the structure-function relationship between SAP and RNFL measurements have formulated quantitative models. [7,13,22–25,28,29] One such model proposes that particular regions of SAP sensitivities are linearly related to RNFL measurements when one considers a given thickness of the RNFL is unchanged at zero sensitivity (a residual RNFL thickness).[13,22,25] Another model that was initially developed for experimental glaucoma in macaque monkeys[7] and, subsequently, modified for normal age-related losses of RGCs in human subjects,[28,29] demonstrated that the neuronal constructs for visual sensitivity for SAP and RNFL thickness from OCT measurements were well correlated when related in terms of ganglion cell populations. However, it must be determined whether the model for RGC losses from normal aging can be applied directly to RGC losses from glaucoma and the present study was an assessment of the nonlinear model relating SAP sensitivity to RNFL thickness to structure-function relationships of patients with glaucoma.

The structure-function model, which has been described previously, is based on the principle that both SAP sensitivity and RNFL thickness are dependent on RGC densities,[7, 26, 27] and can be related directly by a common parameter of RGC numbers. Specifically, visual sensitivity measurements by SAP are considered a reflection of point wise RGC densities and, thus, dependent on retinal eccentricity but not age, while RNFL thicknesses are a function of the RGC axon densities in an age-dependent manner. The prior application of the model produced consistent estimates of RGC populations from SAP and OCT measurements for normal eyes of subjects across five decades of life, with equal accuracy and precision for each decade. Consequently, the normal age-dependent variations in neuronal populations set baselines for the evaluation of pathological alterations caused by glaucoma. This purpose of this experiment is to apply this structure-function relationship model developed in the normative population and tested on normal controls to a group of participants with varying degrees of glaucoma.

Methods

Subjects

Seventy-one subjects from the University Eye Institute, Houston, Texas were included in the study. Control subjects were selected among patient populations, faculty, and students. Glaucoma and glaucoma suspect participants were selected based on having one of the two diagnoses at the time of entrance into the study. The control group was a subset of subjects for the development of the model[29],who were included in the present study to compare to glaucoma-suspects and to determine whether modifications for glaucoma will also affect the

results for normal subjects. For the present study, the control group was comprised of one eye from each of forty subjects (age: 44.8 ± 16.6 years) with no known history of ocular disease or visual field loss and demonstrated no evidence or suspicion of glaucomatous damage with either visual field testing (MD: −0.01 ± 0.08 dB) or OCT measurements of the RNFL (Global thickness: 96.7 ± 10.1 mμ). The glaucomatous group was composed of the worse eye by mean deviation on SAP from thirty-one participants (age: 62.5 ± 15.5 years) diagnosed as either glaucoma or glaucoma suspects by their clinicians (for all patients – MD: −6.74 ± 8.66 dB, global thickness: 77.1 ± 19.4 mμ, Figure 2). In both groups, subjects exhibiting significant media opacity (best corrected visual acuity < 20/40), any visible or past retinal pathology in the posterior pole, or known visual field loss not secondary to glaucoma were excluded from the study. The research adhered to the tenets of the Declaration of Helsinki and the experimental protocol was reviewed and approved by the University of Houston's Committee for the Protection of Human Subjects. Informed consent was obtained from each of the subjects and they were remunerated for their participation.

Clinical Testing

Visual sensitivity was determined for each eye using static threshold perimetry with the Humphrey Visual Field Analyzer II (model 750, Carl Zeiss Meditec, Inc., Dublin, CA). Subjects were tested with 24–2 test pattern using the SITA standard thresholding strategy. Subjects performed two sets of visual fields in one session, with a break between sets, and the second measurements were used for the study. Testing was performed with the standard protocol for visual field testing and only visual field data with reliable test indices (fixation losses < 33% and false positives < 15%) were included in the analysis.

Quantitative measurements of the retinal nerve fiber layer were obtained for each eye using the StratusOCT III (software version 4.0.1 and version 4.0.4, Carl Zeiss Meditec, Inc., Dublin, CA) by one of the authors (NR or JW for control measurements, and JW for glaucoma and glaucoma suspects). The standard 3.4 mm diameter scan for retinal nerve fiber layer thickness was used to obtain 512 measurements along a 10.87 mm circumference scan centered on the optic nerve head. Subjects' pupils were dilated with 1.0% tropicamide prior to OCT testing to ensure adequate image quality (≥6 on all scans). All 512 tomogram measurements from each OCT RNFL thickness scan were then exported for analysis.

Translation of SAP and OCT to ganglion cell estimates

Translation of Perimetry Data to Ganglion Cell Quantities—The methods for conversions of SAP sensitivity to RGC density have been described. [27–30] In brief, the correlation of RGC densities and SAP sensitivities showed that ganglion cell quantity, (*gc*), in decibels at a given retinal location is dependent on the eccentricity from the fovea, (*e*), and the corresponding sensitivity at that visual field test location, (*s*).[27, 30] The equations, as adapted for the human axial length (1.34× longer than the macaque eye), are as follows:

$$m=[(.054\times\{e\times 1.34\})+0.9] \quad 1$$

$$b=[(-1.5\times\{e\times 1.34\})-14.8] \quad 2$$

$$gc=[(\{s-1\}-b)/m]+4.7 \quad 3$$

Where (*m)* is the slope and *(b)* the y-intercept for each eccentricity tested. These functions give the point-location RGC density for each location in the visual field test pattern. In order to find a quantity for a given area, it was assumed that ganglion cell density was uniform for

a given area (6° × 6°) centered on the visual field test location. Therefore, the number of ganglion cells for a given area would be equivalent to the ganglion cell estimate for the test location (unlogged) multiplied by 2.94 (based on the conversion factor that 1 mm retinal distance = 3.5° visual angle for the human eye). One decibel was subtracted from the original sensitivity value for each test location to account for the difference between full threshold testing used in the experimental setting and SITA threshold testing used in the clinical setting.[31, 32]

Translation of OCT measures to Ganglion Cell Axon Quantities—The methods for estimating axonal numbers from RNFL thickness were derived from analyses of the normative rates of decline for SAP sensitivity and RNFL thickness and subsequently applied to normal subjects. The conversion from OCT measures of RNFL thickness to an estimate of RGC axons (*a*) is a linear transformation from the area of RNFL (μm^2) and the density of axons ($a/\mu m^2$), where the area is determined from the OCT thickness measurement and the axon density is a function of the subject's age. [28,29]

$$d=(-0.007\times age)+1.4 \quad 4$$

$$a=\left(\sum_{x}^{x+n} h_x * 21.2\right)\times d \quad 5$$

The total number of axons (*a*) in an OCT scan over a region of pixels from (*x)* to (*x+n)* is determined by the RNFL area, *i.e.,* the height (h_x) of the scan (in μm) at tomogram (*x)* times a constant of 21.2 μm (10.87 mm scan length / 512 pixels per scan) summed across the number of tomograms in the inferior, nasal, or superior region (see Figure 1A), and multiplied by the axon density (*d*) in axons/ μm^2.

Mapping corresponding SAP and OCT locations—Although the previous application of the model mapped the visual field into 10 sectors of the ONH, for this study a more simple approach was used in which the RNFL and visual field were divided into only three regions. The inferior and superior hemifields, each of which encompassed half of the temporal side of the optic nerve head, and a nasal region, which corresponded to the area falling between 144° to 216°.(Figure 1A).[7, 28, 29] In this map, SAP test locations are assigned to one of three areas (Figure 1B), based on the inferior, superior, or nasal region where they would have their axons enter the optic nerve head, but because of the limited SAP data for the nasal sector only the superior and inferior hemifield data were analyzed.

Results

Comparison of SAP and OCT derived estimates

The relationships between the OCT and SAP estimates of neuronal populations for all of the subjects are presented for the superior (Figure 3A) and inferior (Figure 3B) hemifields and both hemifields totaled (Figure 3C). The data for control subjects, glaucoma suspects and glaucoma patients with minimal field loss (i.e., a SAP mean deviation ≥ −3.00 dB) are clustered around the 1:1 line, showing good agreement between the structural and functional estimates. In contrast, the data for patients with more advanced glaucomatous disease show increasing discordance between SAP- and OCT-derived estimates, with the OCT-derived estimates predicting larger RGC populations than the SAP-derived estimates.

Reconciling the discordance between SAP and OCT derived estimates

The discrepancy between OCT and SAP estimates with increasing severity of glaucomatous disease is similar to that observed when a fixed axon density was used and the data were analyzed by age;[28, 29] that is, the difference between estimates is directly proportional to the increase in age or the severity of glaucomatous disease, with the OCT-derived RGC estimates being larger. In the case of aging, the normative data bases for SAP and OCT measurements were used to derive a compensation factor for senescence by opposing changes in the RNFL structure (a decrease in the number of axons with a concurrent decrease in axon density with age). Following a similar strategy, a third quantity, glaucomatous neural loss, was used to make comparisons between the OCT-derived estimates and those derived from SAP. Glaucomatous neural loss is the amount of loss proposed to be lost solely from glaucomatous disease and not from the aging process. Age-expected SAP and OCT estimates were calculated with the following formulas, which were developed in previous experiments relating OCT rates of decline from aging with those from SAP [28, 29]:

$$\text{Age-Expected Axons} = 1260695 - (7047 \times \text{Age}) \quad 7)$$

$$\text{Age-Expected RGCs} = 1240695 - (6145 \times \text{Age}) \quad 8)$$

$$\text{Glaucomatous Neural Loss} = \text{Observed RGCs} - \text{Age-Expected RGCs} \quad 8)$$

Comparison of SAP glaucomatous neural loss and OCT mean neural loss to the mean deviation (MD) index from SAP for each subject demonstrates systematic differences between estimates of neurons as a function of the stage of glaucoma (Figure 3A) Although the calculated glaucomatous neural losses by both structural and functional measurements are directly proportional to the stage of disease as quantified by the perimetric MD, the slope of the function for neuronal losses based on SAP measurements is steeper than for losses determined from OCT estimates. The relationship for the difference in structural and functional estimates as a function of SAP MD gives a correction factor for estimating neural loss from OCT derived measurements for all stages of disease.

$$(sc) = 0.28 \times \text{SAP MD score} - 0.18 \quad 9)$$

Where (*sc)* is the final correction applied to final total estimates from the OCT estimates (in dBs). Figure 3B plots the total estimates from each subject from OCT and SAP for all subjects with the stage-dependent parameter incorporated into the model. With this factor included, the estimates of neuronal populations from SAP and OCT are well correlated with a slope of approximately 1.0.

Discussion

The present study demonstrates that the model developed to relate the systematic changes in SAP and OCT measurements during normal aging was found to applicable to patients with an early stage of glaucoma, but an additional parameter defined by the stage of disease was required to model more advanced disease. Relating SAP sensitivity to OCT RNFL thickness in this model requires that the measurements be compared in terms of their common neural elements, RGCs, by using equations developed in previous experiments.[7, 26–29] RGC quantities as determined by perimetry have been verified histologically in previous experiments, so it seems likely the source of the discrepancy in terms of axonal estimates is

a result of the structural measurement. Given the model's ability to predict equivalent neural elements in the control population when axon density changes as a function of age, the logical choice in determining the discrepancy is to examine the axon density as a function of stage of disease. In both cases, it appears that a decrease in axon density with age and from glaucomatous disease can explain the slower rate of loss from RNFL thickness derived axon estimates when a constant axon density is used. When age and stage of disease are variables incorporated into the OCT-derived estimates, there is excellent agreement with SAP-derived estimates for all subjects.

In a previous investigation,[7] experimental glaucoma was allowed to progress in macaque monkeys in order to develop a quantitative structure-function relationship between OCT RNFL thickness and SAP sensitivity measurements. However, there are important differences in experimental, compared to clinical glaucoma and studies based on the normative databases and non-diseased eyes demonstrated that the age of the subject is an important parameter in calculating axon estimates for OCT RNFL thickness values.[28, 29] Those studies did not address the need for a factor to account for the stage of glaucoma, though, in retrospect, it may have improved agreement in SAP and OCT data for the more advanced field defects in experimental glaucoma, as was demonstrated with the glaucoma patients in this study.

The incorporation of the stage-dependent factor improved the accuracy of the structure-function relationship for moderate to advanced stages of glaucoma. In the present case, the analysis was based on data from entire hemifields in order to reduce inter-subject variability. Previously, the analysis of structural and functional data with a smaller sector-by-sector relationship resulted in greater variability, which would be expected from inter-subject differences in the locations of the regions of maximum thickness in the RNFL.[13] It has also been suggested that SAP is not capable of reliably measuring glaucomatous damage across the entire SAP range due to variability of sensitivity below a certain range[47, 48], and that the dynamic range of measurements from SAP is much smaller, which would negate the need for a stage correction in the later stages of disease since the SAP measurements would be inaccurate in the lower ranges. The inter-subject differences in the RNFL thickness characteristics may also cause variability in mapping the visual field onto the optic nerve head and, thus, greater variability in the analysis of small sections compared to a whole-field analysis. The inter-subject variability of the relationships between visual field and optic nerve data has also been illustrated by recent investigations of the regional relationships.[20, 21, 49, 50]

One possible explanation for the need of a stage corrective factor in the model is glial remodeling of the retinal nerve fiber layer in during the disease process. There is support of remodeling from histological evidence for increased glial tissue found in glaucomatous eyes compared to age-matched control eyes.[51, 52] Gliosis may result in masking the expected rate of decline of RNFL thickness in normal individuals when compared to age-related loss of RGCs, which can help explain the residual RNFL thickness observed in individuals with end-stage glaucomatous visual fields and other optic nerve conditions resulting in death of the axons. Although the model proposes an increase in the non-neural composition of the RNFL both with increasing age and glaucomatous disease, the exact changes that occur need histologic verification.

As an alternative to the model described here, the simple linear model proposed by Hood *et. al.*, [13, 22, 25] relates sensitivity averaged in linear units to RNFL thickness in a corresponding region when the non-axonal elements of the RNFL thickness are held constant (roughly 1/3 of the original thickness value). By this model, a sensitivity of half the normal value on SAP would correspond to a 50% loss of RGCs and their axons, and a 50% loss of RNFL

thickness in the axonal portion of the total thickness, leaving the constant non-axonal portion of thickness the same. The present model predicts that the amount of sensitivity that would correspond with a 50% loss of RGCs and their axons would depend on the eccentricity, but would vary from sensitivity in a logarithmic relationship (i.e., it would take a 3–6 dB loss of sensitivity to account for 50% loss of the ganglion cells), depending on the eccentricity. The nonlinear model also proposes that there would be an increase in the non-axonal components of the RNFL thickness to contribute to the overall thickness of the RNFL as measured by the OCT with both age and increasing stage of disease. Other differences between the linear and nonlinear models have been described in some detail, and although the simple linear model is based on different assumptions, there is support for it in the literature.[53–55]

In conclusion, the study has supported the methods for quantitatively comparing the structural elements of OCT with the functional measurements of SAP in normal subjects and patients with varying stages of glaucomatous disease. At this point, the modifications to account for the stage of glaucoma were developed and tested with data from same population. It is a necessary first step, but it noteworthy that the utility of the model recently was demonstrated for an independent group of patients. The model accurately related structure-function relationships for control subjects, glaucoma suspects, and glaucoma patients with early- to late-stage disease and, therefore, argues against the concepts of perimetric defects preceding anatomical defects, or vice versa. Future development will be undertaken for applying the stage of disease correction to individual test locations and sectors as they are likely to vary at different locations around the optic nerve head. This structure-function model might also be strengthened by correlating these measurements with other structural measurements (particularly scanning laser polarimetry of the retinal nerve fiber layer). Lastly, histological studies are needed to determine whether RNFL composition changes in response to both the aging process and to glaucomatous disease.

Acknowledgments

The work was supported by grants R01 EY001139, P30 EY007551, T32 EY007024, and K23 EY018329 from the National Eye Institute and a John and Rebecca Moores Professorship from the University of Houston.

Support: NIH grants: R01 EY001139, P30 EY007751, T32 EY007024, and K23 EY018329 and a John and Rebecca Moores Professorship from the University of Houston.

References

1. Bowd C, Weinreb RN, Williams JM, Zangwill LM. The retinal nerve fiber layer thickness in ocular hypertensive, normal, and glaucomatous eyes with optical coherence tomography. Arch Ophthalmol. 2000; 118:22–26. [PubMed: 10636409]
2. Sommer A, Pollack I, Maumenee AE. Optic disc parameters and onset of glaucomatous field loss. II. Static screening criteria. Arch Ophthalmol. 1979; 97:1449–1454. [PubMed: 464867]
3. Sommer A, Pollack I, Maumenee AE. Optic disc parameters and onset of glaucomatous field loss. I. Methods and progressive changes in disc morphology. Arch Ophthalmol. 1979; 97:1444–1448. [PubMed: 464866]
4. Sommer A, Katz J, Quigley HA, et al. Clinically detectable nerve fiber atrophy precedes the onset of glaucomatous field loss. Arch Ophthalmol. 1991; 109:77–83. [PubMed: 1987954]
5. Kass MA, Heuer DK, Higginbotham EJ, et al. The Ocular Hypertension Treatment Study: a randomized trial determines that topical ocular hypotensive medication delays or prevents the onset of primary open-angle glaucoma. Arch Ophthalmol. 2002; 120:701–713. discussion 829–730. [PubMed: 12049574]
6. Miglior S, Zeyen T, Pfeiffer N, Cunha-Vaz J, Torri V, Adamsons I. Results of the European Glaucoma Prevention Study. Ophthalmology. 2005; 112:366–375. [PubMed: 15745761]

7. Harwerth RS, Vilupuru AS, Rangaswamy NV, Smith EL 3rd. The relationship between nerve fiber layer and perimetry measurements. Invest Ophthalmol Vis Sci. 2007; 48:763–773. [PubMed: 17251476]
8. Wollstein G, Schuman JS, Price LL, et al. Optical coherence tomography longitudinal evaluation of retinal nerve fiber layer thickness in glaucoma. Arch Ophthalmol. 2005; 123:464–470. [PubMed: 15824218]
9. Quigley HA, Dunkelberger GR, Green WR. Retinal ganglion cell atrophy correlated with automated perimetry in human eyes with glaucoma. Am J Ophthalmol. 1989; 107:453–464. [PubMed: 2712129]
10. Harwerth RS, Carter-Dawson L, Shen F, Smith EL 3rd, Crawford ML. Ganglion cell losses underlying visual field defects from experimental glaucoma. Invest Ophthalmol Vis Sci. 1999; 40:2242–2250. [PubMed: 10476789]
11. Bach M, Hoffmann MB. Update on the pattern electroretinogram in glaucoma. Optom Vis Sci. 2008; 85:386–395. [PubMed: 18521020]
12. Buckingham BP, Inman DM, Lambert W, et al. Progressive ganglion cell degeneration precedes neuronal loss in a mouse model of glaucoma. J Neurosci. 2008; 28:2735–2744. [PubMed: 18337403]
13. Hood DC, Kardon RH. A framework for comparing structural and functional measures of glaucomatous damage. Prog Retin Eye Res. 2007; 26:688–710. [PubMed: 17889587]
14. Schuman JS, Hee MR, Puliafito CA, et al. Quantification of nerve fiber layer thickness in normal and glaucomatous eyes using optical coherence tomography. Arch Ophthalmol. 1995; 113:586–596. [PubMed: 7748128]
15. Heijl, A.; Patella, V. Essential Perimetry: The Field Analyzer Primer. 3. Carl Zeiss Meditec; 2002.
16. Ghadiali Q, Hood DC, Lee C, et al. An analysis of normal variations in retinal nerve fiber layer thickness profiles measured with optical coherence tomography. J Glaucoma. 2008; 17:333–340. [PubMed: 18703941]
17. Patella, V. StratusOCT: Establishment of Normative Reference Values for Retinal Nerve Fiber Layer Thickness Measurements. Dublin, CA: Carl Zeiss Meditec, Inc; 2003.
18. Budenz DL, Anderson DR, Varma R, et al. Determinants of normal retinal nerve fiber layer thickness measured by Stratus OCT. Ophthalmology. 2007; 114:1046–1052. [PubMed: 17210181]
19. Garway-Heath DF, Poinoosawmy D, Fitzke FW, Hitchings RA. Mapping the visual field to the optic disc in normal tension glaucoma eyes. Ophthalmology. 2000; 107:1809–1815. [PubMed: 11013178]
20. Strouthidis NG, Vinciotti V, Tucker AJ, Gardiner SK, Crabb DP, Garway-Heath DF. Structure and function in glaucoma: The relationship between a functional visual field map and an anatomic retinal map. Invest Ophthalmol Vis Sci. 2006; 47:5356–5362. [PubMed: 17122124]
21. Ferreras A, Pablo LE, Garway-Heath DF, Fogagnolo P, Garcia-Feijoo J. Mapping standard automated perimetry to the peripapillary retinal nerve fiber layer in glaucoma. Invest Ophthalmol Vis Sci. 2008; 49:3018–3025. [PubMed: 18378581]
22. Hood DC, Anderson SC, Wall M, Kardon RH. Structure versus function in glaucoma: an application of a linear model. Invest Ophthalmol Vis Sci. 2007; 48:3662–3668. [PubMed: 17652736]
23. El Beltagi TA, Bowd C, Boden C, et al. Retinal nerve fiber layer thickness measured with optical coherence tomography is related to visual function in glaucomatous eyes. Ophthalmology. 2003; 110:2185–2191. [PubMed: 14597528]
24. Bowd C, Zangwill LM, Medeiros FA, et al. Structure-function relationships using confocal scanning laser ophthalmoscopy, optical coherence tomography, and scanning laser polarimetry. Invest Ophthalmol Vis Sci. 2006; 47:2889–2895. [PubMed: 16799030]
25. Hood DC. Relating retinal nerve fiber thickness to behavioral sensitivity in patients with glaucoma: application of a linear model. J Opt Soc Am A Opt Image Sci Vis. 2007; 24:1426–1430. [PubMed: 17429489]
26. Harwerth RS, Crawford ML, Frishman LJ, Viswanathan S, Smith EL 3rd, Carter-Dawson L. Visual field defects and neural losses from experimental glaucoma. Prog Retin Eye Res. 2002; 21:91–125. [PubMed: 11906813]

27. Harwerth RS, Quigley HA. Visual field defects and retinal ganglion cell losses in patients with glaucoma. Arch Ophthalmol. 2006; 124:853–859. [PubMed: 16769839]
28. Harwerth RS, Wheat JL. Modeling the effects of aging on retinal ganglion cell density and nerve fiber layer thickness. Graefes Arch Clin Exp Ophthalmol. 2008; 246:305–314. [PubMed: 17934750]
29. Harwerth RS, Wheat JL, Rangaswamy NV. Age-Related Losses of Retinal Ganglion Cells and Axons. Invest Ophthalmol Vis Sci. 2008 Oct; 49(10):4437–43. [PubMed: 18539947]
30. Harwerth RS, Carter-Dawson L, Smith EL 3rd, Barnes G, Holt WF, Crawford ML. Neural losses correlated with visual losses in clinical perimetry. Invest Ophthalmol Vis Sci. 2004; 45:3152–3160. [PubMed: 15326134]
31. Artes PH, Iwase A, Ohno Y, Kitazawa Y, Chauhan BC. Properties of perimetric threshold estimates from Full Threshold, SITA Standard, and SITA Fast strategies. Invest Ophthalmol Vis Sci. 2002; 43:2654–2659. [PubMed: 12147599]
32. Bengtsson B, Heijl A. Evaluation of a new perimetric threshold strategy, SITA, in patients with manifest and suspect glaucoma. Acta Ophthalmol Scand. 1998; 76:268–272. [PubMed: 9686835]
33. Blanks JC, Schmidt SY, Torigoe Y, Porrello KV, Hinton DR, Blanks RH. Retinal pathology in Alzheimer's disease. II. Regional neuron loss and glial changes in GCL. Neurobiol Aging. 1996; 17:385–395. [PubMed: 8725900]
34. Harman A, Abrahams B, Moore S, Hoskins R. Neuronal density in the human retinal ganglion cell layer from 16–77 years. Anat Rec. 2000; 260:124–131. [PubMed: 10993949]
35. Kerrigan-Baumrind LA, Quigley HA, Pease ME, Kerrigan DF, Mitchell RS. Number of ganglion cells in glaucoma eyes compared with threshold visual field tests in the same persons. Invest Ophthalmol Vis Sci. 2000; 41:741–748. [PubMed: 10711689]
36. Balazsi AG, Rootman J, Drance SM, Schulzer M, Douglas GR. The effect of age on the nerve fiber population of the human optic nerve. Am J Ophthalmol. 1984; 97:760–766. [PubMed: 6731540]
37. Repka MX, Quigley HA. The effect of age on normal human optic nerve fiber number and diameter. Ophthalmology. 1989; 96:26–32. [PubMed: 2919049]
38. Mikelberg FS, Drance SM, Schulzer M, Yidegiligne HM, Weis MM. The normal human optic nerve. Axon count and axon diameter distribution. Ophthalmology. 1989; 96:1325–1328. [PubMed: 2780002]
39. Jonas JB, Schmidt AM, Muller-Bergh JA, Schlotzer-Schrehardt UM, Naumann GO. Human optic nerve fiber count and optic disc size. Invest Ophthalmol Vis Sci. 1992; 33:2012–2018. [PubMed: 1582806]
40. Blanks JC, Torigoe Y, Hinton DR, Blanks RH. Retinal pathology in Alzheimer's disease. I. Ganglion cell loss in foveal/parafoveal retina. Neurobiol Aging. 1996; 17:377–384. [PubMed: 8725899]
41. Kanamori A, Escano MF, Eno A, et al. Evaluation of the effect of aging on retinal nerve fiber layer thickness measured by optical coherence tomography. Ophthalmologica. 2003; 217:273–278. [PubMed: 12792133]
42. Alamouti B, Funk J. Retinal thickness decreases with age: an OCT study. Br J Ophthalmol. 2003; 87:899–901. [PubMed: 12812895]
43. Varma R, Bazzaz S, Lai M. Optical tomography-measured retinal nerve fiber layer thickness in normal latinos. Invest Ophthalmol Vis Sci. 2003; 44:3369–3373. [PubMed: 12882783]
44. Sony P, Sihota R, Tewari HK, Venkatesh P, Singh R. Quantification of the retinal nerve fibre layer thickness in normal Indian eyes with optical coherence tomography. Indian J Ophthalmol. 2004; 52:303–309. [PubMed: 15693322]
45. Ramakrishnan R, Mittal S, Ambatkar S, Kader MA. Retinal nerve fibre layer thickness measurements in normal Indian population by optical coherence tomography. Indian J Ophthalmol. 2006; 54:11–15. [PubMed: 16531664]
46. Salchow DJ, Oleynikov YS, Chiang MF, et al. Retinal nerve fiber layer thickness in normal children measured with optical coherence tomography. Ophthalmology. 2006; 113:786–791. [PubMed: 16650674]
47. Heijl A, Lindgren A, Lindgren G. Test-retest variability in glaucomatous visual fields. Am J Ophthalmol. 1989; 108:130–135. [PubMed: 2757094]

48. Wall M, Woodward KR, Doyle CK, Artes PH. Repeatability of automated perimetry: a comparison between standard automated perimetry with stimulus size III and V, matrix, and motion perimetry. Invest Ophthalmol Vis Sci. 2009; 50:974–979. [PubMed: 18952921]

49. Gardiner SK, Johnson CA, Cioffi GA. Evaluation of the structure-function relationship in glaucoma. Invest Ophthalmol Vis Sci. 2005; 46:3712–3717. [PubMed: 16186353]

50. Kanamori A, Naka M, Nagai-Kusuhara A, Yamada Y, Nakamura M, Negi A. Regional relationship between retinal nerve fiber layer thickness and corresponding visual field sensitivity in glaucomatous eyes. Arch Ophthalmol. 2008; 126:1500–1506. [PubMed: 19001216]

51. Wang L, Cioffi GA, Cull G, Dong J, Fortune B. Immunohistologic evidence for retinal glial cell changes in human glaucoma. Invest Ophthalmol Vis Sci. 2002; 43:1088–1094. [PubMed: 11923250]

52. Varela HJ, Hernandez MR. Astrocyte responses in human optic nerve head with primary open-angle glaucoma. J Glaucoma. 1997; 6:303–313. [PubMed: 9327349]

53. Garway-Heath DF, Caprioli J, Fitzke FW, Hitchings RA. Scaling the hill of vision: the physiological relationship between light sensitivity and ganglion cell numbers. Invest Ophthalmol Vis Sci. 2000; 41:1774–1782. [PubMed: 10845598]

54. Garway-Heath DF, Holder GE, Fitzke FW, Hitchings RA. Relationship between electrophysiological, psychophysical, and anatomical measurements in glaucoma. Invest Ophthalmol Vis Sci. 2002; 43:2213–2220. [PubMed: 12091419]

55. Swanson WH, Felius J, Pan F. Perimetric defects and ganglion cell damage: interpreting linear relations using a two-stage neural model. Invest Ophthalmol Vis Sci. 2004; 45:466–472. [PubMed: 14744886]

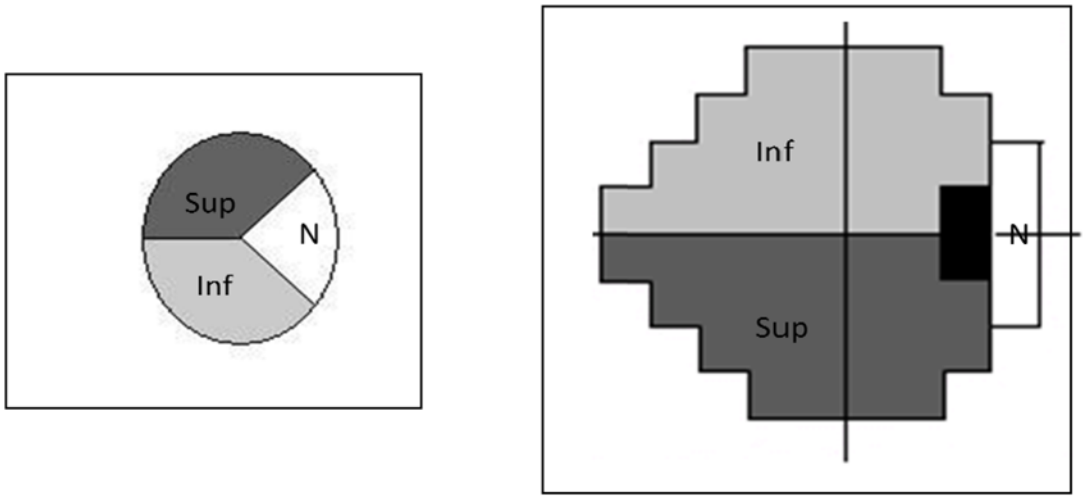

Figure 1.
Sector assignment for SAP test locations and the OCT RNFL scan. Figure 1 shows the visual field test locations and the corresponding RNFL assignment.

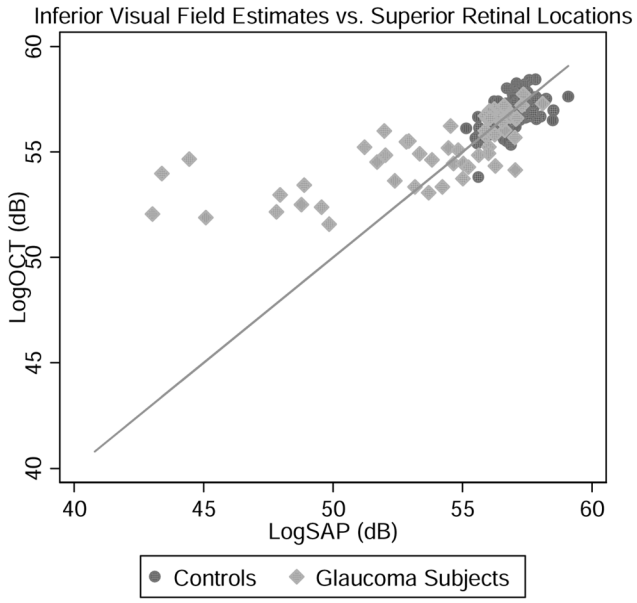

A.

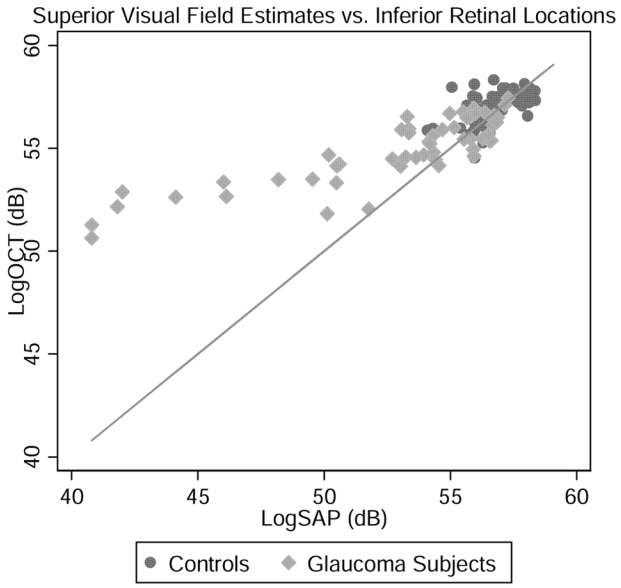

B.

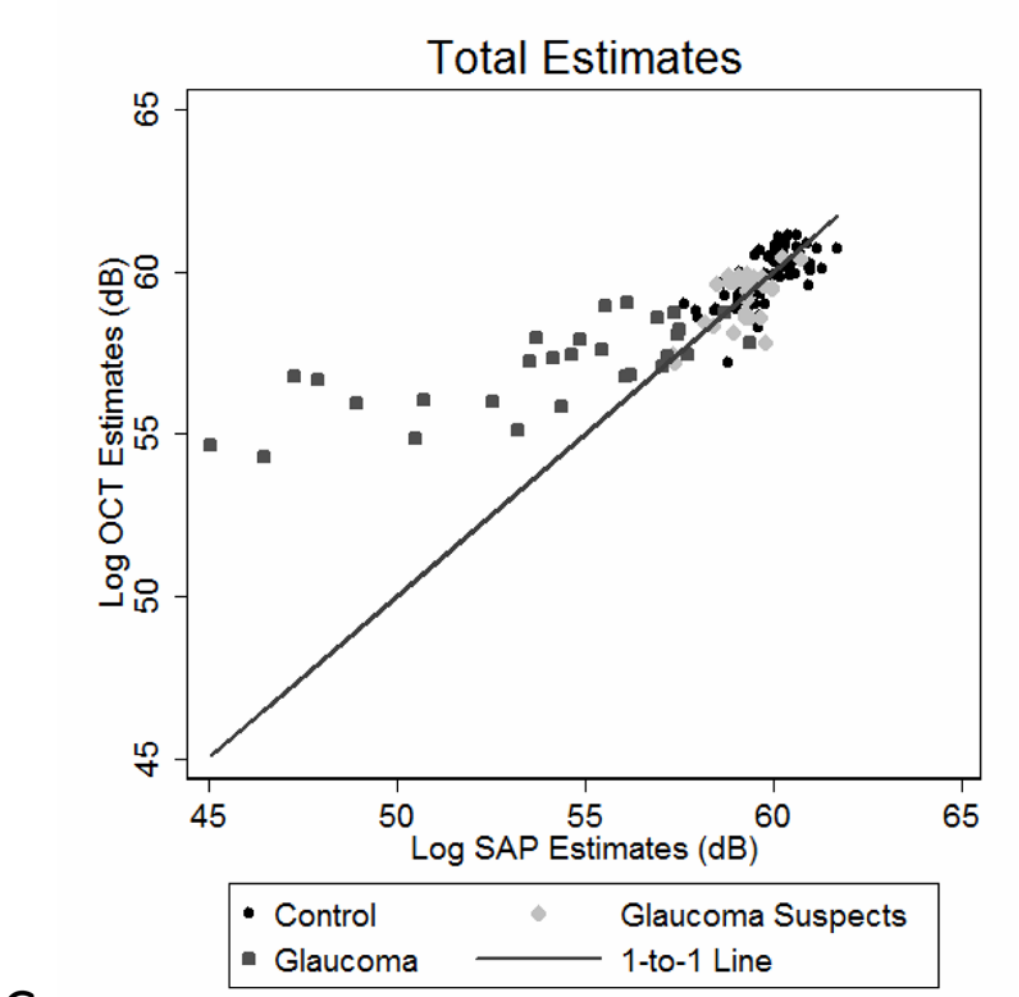

C.

Figure 2.

Inferior visual field vs. Superior OCT derived RGC estimates (A), Superior visual fields and Inferior OCT estimates (B), and total estimates (C) of RGC's/axons from SAP and OCT measurements for all subjects. The solid line represents the one-to-one line. All appear to reveal agreement in normal and early glaucomatous damage, with increasing discordance between estimates with increasing glaucomatous damage.

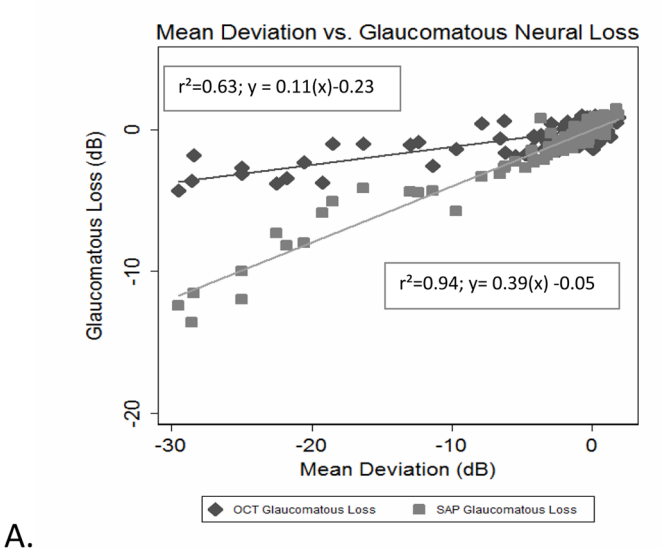

A.

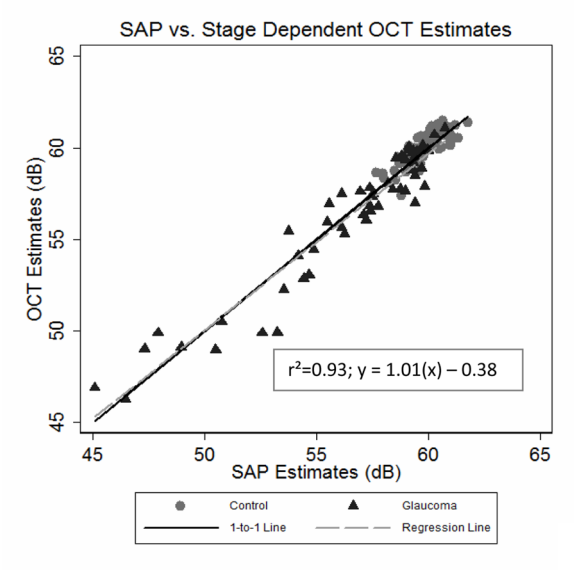

B.

Figure 3.

Glaucomatous neural loss as a function of SAP Mean Deviation (A) and SAP Totals versus OCT totals with stage of disease compensation for OCT estimates(B). (A) shows the relationships between disease severity (measured from Mean Deviation with SAP) and glaucomatous neural loss (Observed OCT estimate – expected OCT estimate for OCT-derived measures and Observed SAP estimate – expected age SAP estimate for SAP-derived measures) for each subject. (B) shows the total estimates with stage of disease correction, revealing conformity for all subjects, when the correction for stage of disease is applied to the final estimates.

Table 1

Subject characteristics for glaucoma suspects and glaucoma groups combined.
Visual field and RNFL characteristics of glaucomatous group.

SUBJECT	AGE	MD (dB) OD	MD(db) OS	Average RNFL Thickness(μm) OD	Average RNFL Thickness(μm) OS
Mean	61.6	−7.78	−5.99	75.26	77.45
Std. Dev.	15.8	10.09	7.61	19.40	18.40
Min	32	−29.50	−26.77	41.01	44.54
Max	85	0.95	1.90	110.63	113.63